Earth and Planetary Science Letters 525 (2019) 115763

Contents lists available at ScienceDirect

Earth and Planetary Science Letters

www.elsevier.com/locate/epsl

# Variable modification of continental lithosphere during the Proterozoic Grenville orogeny: Evidence from teleseismic P-wave tomography ☆

Alistair Boyce [a,*,1], Ian D. Bastow [a], Eva M. Golos [b], Stéphane Rondenay [c], Scott Burdick [d], Robert D. Van der Hilst [b]

[a] Department of Earth Science and Engineering, Royal School of Mines, Prince Consort Road, Imperial College London, London, SW7 2BP, UK
[b] Department of Earth, Atmospheric and Planetary Sciences, Massachusetts Institute of Technology, Cambridge, MA, USA
[c] Department of Earth Science, University of Bergen, Allegaten 41, 5007 Bergen, Norway
[d] Department of Geology, Wayne State University, Detroit, MI, 48202, USA

ARTICLE INFO

*Article history:*
Received 19 February 2019
Received in revised form 5 August 2019
Accepted 7 August 2019
Available online xxxx
Editor: M. Ishii

*Keywords:*
absolute arrival-times
P-wave tomography
Precambrian North America
Grenville orogeny
cratonic modification
metasomatism

ABSTRACT

Cratons, the ancient cores of the continents, have survived thermal and mechanical erosion over multiple Wilson cycles, but the ability of their margins to withstand modification during continental convergence is debated. The Proterozoic Grenville orogeny operated for ≥300 Myr along the eastern edge of the proto-North American continent Laurentia, whose age varied north-to-south from ~1.5–0.25 Gyr at the time of collision. The preserved Grenville Province, west of the Appalachian terranes, has remained largely tectonically quiescent since its formation. Thick, cool, mantle lithosphere that underlies these Proterozoic regions is typically identified by elevated seismic velocities but lithospheric modification by fluid/melt-derived metasomatic enrichment above a subduction zone, can lead to a reduction in $V_P$ with little effect on $V_S$ and density. Absolute P-wavespeed constraints are therefore a vital complement to existing S-wave tomographic models of North America to investigate craton edge modification mechanisms in the Grenville orogen.

New P-wave tomographic imaging of the North American continent, which benefits from recent developments in arrival-time processing of regional network deployments from the Canadian shield, reveals along strike wavespeed variation in the Grenville orogen. In the north, high seismic wavespeeds (to depths of 250 km) extend eastwards, from the Archean core of North America to beneath the Canadian Grenville Province. In contrast, below the southern U.S., high lithospheric wavespeeds are restricted to west of the Grenville Province, in particular at depths less than 150 km. We argue that subduction-derived metasomatism beneath eastern Laurentia modified the southern Grenville, prior to thermal stabilization and perhaps mantle keel formation. Beneath the northern Grenville, the thick, depleted Laurentian lithosphere resisted extensive metasomatism. Along strike age differences in Grenvillian terranes and their resulting metasomatic modification histories suggests that at least 250 Myr is required for Proterozoic lithosphere to gain resistance to modification.



## 1. Introduction

### 1.1. Background

The cratonic cores of the continents have resisted thermal and mechanical erosion since their formation in the Archean (≥2.5 Ga). Their thick (≥250 km), buoyant, iron-depleted mantle keels or roots (Jordan, 1978; Hawkesworth et al., 1990) are perhaps twenty times more viscous than normal mantle (Sleep, 2003). Such mantle keels, when combined with a strong crust (Jackson et al., 2008), contribute to cratonic longevity. However, the surrounding Proterozoic terranes, which often shield the cratons from tectonic collisions, are expected to be affected by subduction and orogene-

☆ The authors have no conflicting interests to declare.

* Corresponding author.
*E-mail addresses:* ab2568@cam.ac.uk (A. Boyce), i.bastow@imperial.ac.uk (I.D. Bastow), emgolos@mit.edu (E.M. Golos), Rondenay@uib.no (S. Rondenay), sburdick@wayne.edu (S. Burdick), hilst@mit.edu (R.D. Van der Hilst).
[1] Present address: University of Cambridge, Department of Earth Science, Bullard Laboratories, Madingley Road, Cambridge, CB3 0EZ, UK.

https://doi.org/10.1016/j.epsl.2019.115763
0012-821X/

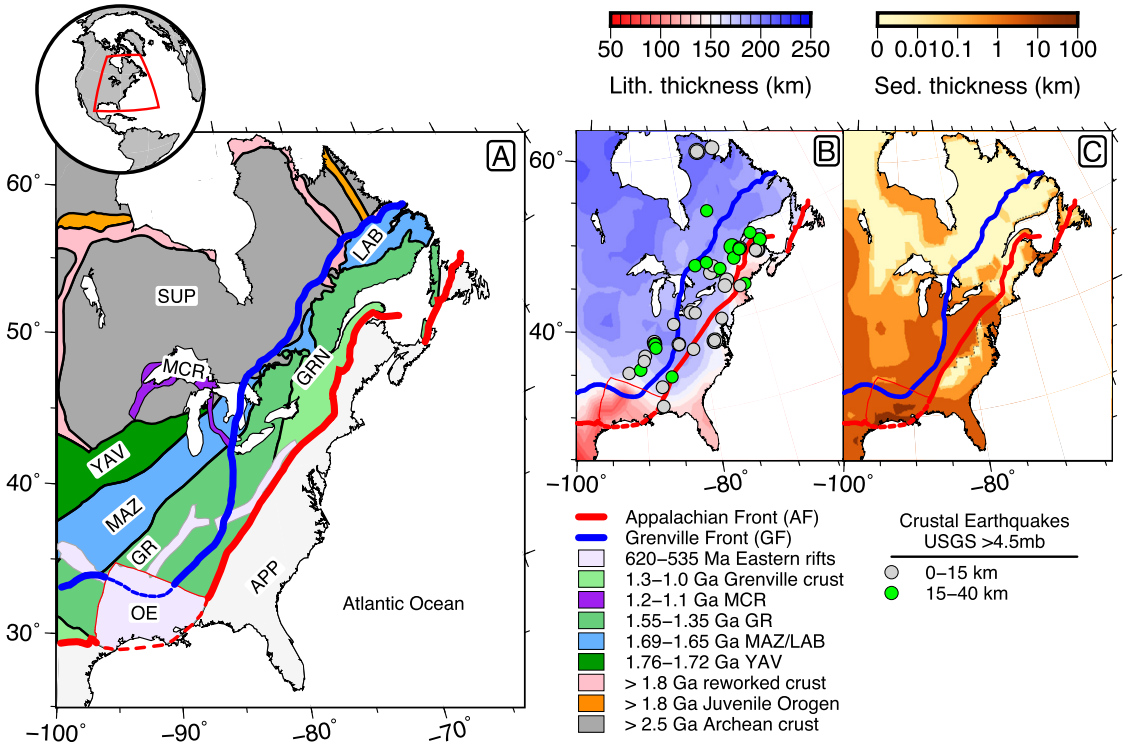


**Fig. 1.** Geological setting. A.) Simplified Precambrian geology of eastern North America (adapted from Whitmeyer and Karlstrom, 2007). In the north, Archean rocks of the Superior (SUP) underthrust the Grenville Province (GRN) (Ludden and Hynes, 2000). The northern Grenville crust is formed of Labradorian (LAB - 1.68–1.65 Ga), Granite-Rhyolite (GR - 1.55–1.35 Ga) and 1.3–1.0 Ga crust, reworked during the Grenville orogen. To the south, the U.S. Mid-Continent is formed from Paleoproterozoic Yavapai (YAV - 1.76–1.72 Ga), Mazatzal (MAZ - 1.69–1.65 Ga) and Granite-Rhyolite (GR - 1.55–1.35 Ga) constituents, whilst the adjacent southern Grenville Province is formed of mostly Granite-Rhyolite material. The failed Mid-Continent rift (MCR) cross-cut these terranes at 1.2–1.1 Ga. The Grenville (blue) and Appalachian (red) tectonic deformation fronts are shown as thick lines. The location of Appalachian terranes (APP) is also indicated. Light purple regions in the south show failed rift basins (620–535 Ma) associated with rifting of Rodinia and later, the Argentine Precordillera that formed the Ouachita Embayment (OE). B.) Lithospheric thickness map of eastern North America after Priestley et al. (2019). Shallow (grey) and deeper (green) crustal continental earthquakes from the USGS catalogue $\geq 4.5 m_b$ are also shown. C.) Sediment thickness map of eastern North America from Laske and Masters (1997). Rocks outcrop in Canadian Grenville but subcrop south of the Great Lakes in the U.S. (For interpretation of the colors in the figure(s), the reader is referred to the web version of this article.)

sis during multiple episodes of continental rifting and subsequent convergence known as Wilson cycles.

The Grenville orogeny of North America extended more than 4000 km along the eastern margin of the Proterozoic Laurentian continent. Active between 1.3 and 1.0 Ga, it was unusually temporally protracted compared to modern orogens that are typically active for less than 100 Myr (Rivers, 2009). The Grenville collision comprised multiple Precambrian terranes of varying age along strike (Fig. 1; Whitmeyer and Karlstrom, 2007). During collision, the northern Laurentian margin was up to ~1.5 Gyr old, while the southern margin was less than 250 Myr old (Whitmeyer and Karlstrom, 2007). Preserved today as thick lithosphere (~200 km e.g., Priestley et al., 2019) far from active plate boundary tectonism, the Grenville is an ideal locale to study craton margin modification during the Proterozoic.

Processes capable of modifying 'stable' lithosphere are legion. Continental lithosphere may be modified by hotspot tectonism (e.g., Boyce et al., 2016), erosion or thinning (e.g., Frederiksen et al., 2013; Liao et al., 2017), basal drag from viscous mantle flow (e.g., Eaton and Frederiksen, 2007) and gravitational destabilization (e.g., Harig et al., 2010). Specifically at continental margins, subduction may also lead to the modification of cratonic lithosphere (e.g., Boyce et al., 2016; Currie and Wijk, 2016) and adjacent continental lithosphere (e.g., Bao et al., 2014). By addition of orthopyroxene derived from silica-rich fluids and/or melt (Schutt and Lesher, 2010), depleted mantle lithosphere above a downgoing slab can be modified by metasomatism (e.g., Kelemen et al., 1998; Wagner et al., 2008; Chiarenzelli et al., 2010; Boyce et al., 2016). Cool, depleted mantle lithosphere typically exhibits high seismic wavespeeds (e.g., Schutt and Lesher, 2006), but such metasomatism likely reduces $V_P$ with little impact on $V_S$ and density (Wagner et al., 2008; Schutt and Lesher, 2010). Metasomatism is considered necessary to explain decreased lithospheric $V_P/V_S$ ratios above the present-day Peru-Chile Trench subduction zone, regardless of the depletion level of the overriding mantle lithosphere (Wagner et al., 2008). Whilst shear velocities are relatively well constrained below the North American continent (e.g., Schaeffer and Lebedev, 2014), critically lacking is a continental-scale P-wave seismic image capable of sampling the Grenvillian mantle lithosphere with adequate lateral resolution to assess the impact of modification at the craton margin.

Here we develop a new P-wave tomographic model of the North American continent (BBNAP19) using data derived from regional networks in southeast Canada (Boyce et al., 2016), processed using the absolute arrival-time recovery method (AARM; Boyce et al., 2017), to supplement P-wave data from a global database and USArray (Li et al., 2008a; Burdick et al., 2017). The regional networks in Canada include, but are not limited to, the Canadian National Seismograph Network (CNSN), the Portable Observatories for Lithospheric Analysis and Research Investigating Seismicity (POLARIS) and the Deep Structure of Three Continental Sutures Québec-Maine Array (QM-III) networks (Darbyshire et al., 2017). These new data enable resolution of Earth structure northwards into the Canadian lithosphere. Specifically, we aim to use our P-wave images to constrain the extent of lithospheric modification via subduction-induced metasomatism prior to terminal continental collision in Proterozoic times.

### 1.2. Geological overview

The 2.6−3.6 Ga Superior craton forms the core of the Canadian Shield (Fig. 1). It exposes the largest continuous area of Archean rocks on Earth today (Card, 1990), which once formed a substantial part of the proto-North American continent of Laurentia. To the south, the Superior witnessed numerous continent-arc collisions and accretion from 1.8−1.3 Ga (Whitmeyer and Karlstrom, 2007). These led to the formation of the Yavapai Province at 1.76−1.72 Ga, Mazatzal and Labradorian Provinces from 1.69−1.65 Ga, and the Granite-Rhyolite Province (from 1.55−1.35 Ga; Fig. 1). Presently, these terranes are covered by Paleozoic sediments in the U.S. but outcrop in Canada (Fig. 1; Laske and Masters, 1997). In the east, the subsequent continent-continent collisions during the Grenville orogeny (1.3−0.9 Ga) resulted in the formation of Rodinia (Li et al., 2008b). Laurentia was affected by multiple phases of compression and extension during the Grenville orogeny. These included the Elzeverian (1.3−1.2 Ga) and Ottawan (1.09−0.98 Ga) orogenic phases (Rivers, 2009). Laurentia is thought to have collided with Amazonia during this period (Li et al., 2008b), but the more than 4000 km long Grenville collision zone may have comprised up to four cratonic blocks (N-S: Baltica, Amazonia, Congo, Kalahari), although precise constraints are lacking (Hoffman, 1991).

The present-day surface expression of the orogen is bound by the Grenville deformation front (GF) to the west and the Appalachian front (AF) in the east (Fig. 1). However, the recent study of Stein et al. (2017) proposed that gravity anomalies, co-located with the GF in the U.S. relate to the failed 1.2−1.1 Ga Mid-Continent rift (Fig. 1); they contend that the Grenville deformation front may not be a lithospheric feature anywhere in the U.S.

At the Superior's southeastern margin, an 'Andean-style' subduction system (Rivers, 1997), dipping to the present-day northwest, may have operated for more than 300 Myr, leading to the metasomatic enrichment of the Grenvillian mantle (Chiarenzelli et al., 2010). A subsequent phase of subduction in the opposing direction (Ludden and Hynes, 2000) may have accreted the Proterozoic island arcs and other fragments of continental and oceanic affiliation to the edge of the Superior craton. Today, approximately coeval, petrologically similar, post-orogenic granites are observed at the surface throughout the Grenville Province (Davidson, 1995; Whitmeyer and Karlstrom, 2007).

The supercontinent Rodinia broke up at 0.62−0.55 Ga (Whitmeyer and Karlstrom, 2007; Li et al., 2008b), forming the Iapetus Ocean. The elongate rift basins that cross-cut the GF in the southeastern U.S. formed during this period, along with the Ouachita Embayment. The Iapetus ocean and subsequent Rheic ocean closed at 0.46−0.26 Ga (Hatcher, 2005), terminating in the Appalachian orogeny to the southeast of the Grenville Province forming Pangea. Rifting of Pangea began to open the Atlantic Ocean at ∼180 Ma. Excluding the Appalachian orogeny, the only known major Phanerozoic tectonic events to have affected eastern North America are related to localized magmatism; the Mesozoic passage of the Great Meteor hotspot (ca. 190−110 Ma; Heaman and Kjarsgaard, 2000) and the Cenozoic volcanism in Virginia at 48 Ma (Mazza et al., 2014).

### 1.3. Previous seismic studies of Proterozoic North America

Global seismic models show the Canadian shield is dominated by high seismic velocities ($\delta V_S$>4%, $\delta V_P$>1%) at lithospheric depths (e.g., Li et al., 2008a; Priestley et al., 2019). Li et al. (2008a) show two high velocity regions ($\delta V_P \sim +1.5\%$) in the southern Granite-Rhyolite and Mazatzal Provinces and a wide NW-SE trending low velocity anomaly ($\delta V_P \sim -1.0\%$) centered around 40°N crossing the Appalachian front. The easterly extent of high wavespeeds does not appear to show correlation with Proterozoic terrane boundaries (Fig. 1).

Continental body wave studies of North America also show consistently high velocities in the Precambrian continental interior (e.g., Schmandt and Lin, 2014; Burdick et al., 2017). Schmandt and Lin (2014) show the highest lithospheric wavespeeds to stretch from the Precambrian rifted margin at ∼105°W to the Appalachian front, east of which is dominated by low velocity anomalies, most notably the central and northern Appalachian anomalies at ∼38°N, 78°W and ∼43°N, 72°W. However, Burdick et al. (2017) show the highest velocities to be generally confined to the Mesoproterozoic domains of the central U.S.; the younger eastern terranes are characterized by pervasive low amplitude high velocity anomalies and localized low velocity anomalies.

Continental surface wave models (e.g., Schaeffer and Lebedev, 2014) also show high velocities beneath the North American shield. In Canada, elevated wavespeeds exist throughout the lithosphere (∼250 km) in the Archean Superior Province and extend into the Proterozoic Grenville at upper lithospheric depths (≤100 km; Schaeffer and Lebedev, 2014). The Mesoproterozoic regions of the central U.S. exhibit slightly lower shear velocities than within the Archean Superior craton to the north (Schaeffer and Lebedev, 2014). High shear wavespeeds gradually decrease eastward through the Grenville and Appalachians in the U.S.

In Canada, regional relative arrival-time body wave imaging (Boyce et al., 2016) shows a velocity decrease between the Archean and Proterozoic domains in the upper mantle. A similar study in the U.S. (Biryol et al., 2016), shows high wavespeeds to extend eastward of the GF, to ∼84−82°W, in the upper-most mantle (≤130 km) but are restricted to west of the GF at ∼86−84°W at greater depths (≤250 km). Surface wave studies in both Canada and the U.S. (Pollitz and Mooney, 2016; Petrescu et al., 2017) show shear velocities generally decrease east of the GF, but an abrupt wavespeed boundary co-incident with the GF is not observed. Hence, high shear velocities are not restricted to the Precambrian terranes west of the GF throughout eastern North America. Wide-angle seismic experiments show Grenvillian rocks are thrust on top of older Archean Superior rocks for more than 300 km at the GF in Canada (Ludden and Hynes, 2000), whilst crustal faulting in the U.S. only involved younger Proterozoic material (Hauser, 1993).

Owing to resolution constraints (greater vertical for surface waves, greater lateral for body waves) and varying data coverage between models, agreement between shear and compressional wave tomographic models is often lacking. By extending absolute P-wave velocity constraints into Canada, we can offer first-order comparisons to existing surface wave models for the entire Grenville Province. Any inferred anti-correlation between shear and compressional velocities in the Grenville Province may therefore be less dominated by data coverage, but more likely, from differing thermochemical sensitivities of $V_S$ and $V_P$ (Wagner et al., 2008; Schutt and Lesher, 2010). Our tomographic model will also help resolve the recently-debated issue of whether Grenvillian tectonic processes operated in the eastern U.S. lithosphere (Stein et al., 2017).

## 2. Data and methods

### 2.1. Global and continental datasets

Our global dataset of absolute arrival-time picks includes P, PP, Pn, Pg, pP, PKP, PKiKP and PKIKP phases from the "EHB" database (Engdahl et al., 1998) spanning the period 1964−2007 (Li et al., 2008a). We supplement the global dataset with the USArray Transportable Array (TA) (e.g., Burdick et al., 2017) which provides absolute arrival-time residuals for P, Pn, PP, PKP, PKiKP and PKIKP phases for 24288 earthquakes recorded between April 2004 and

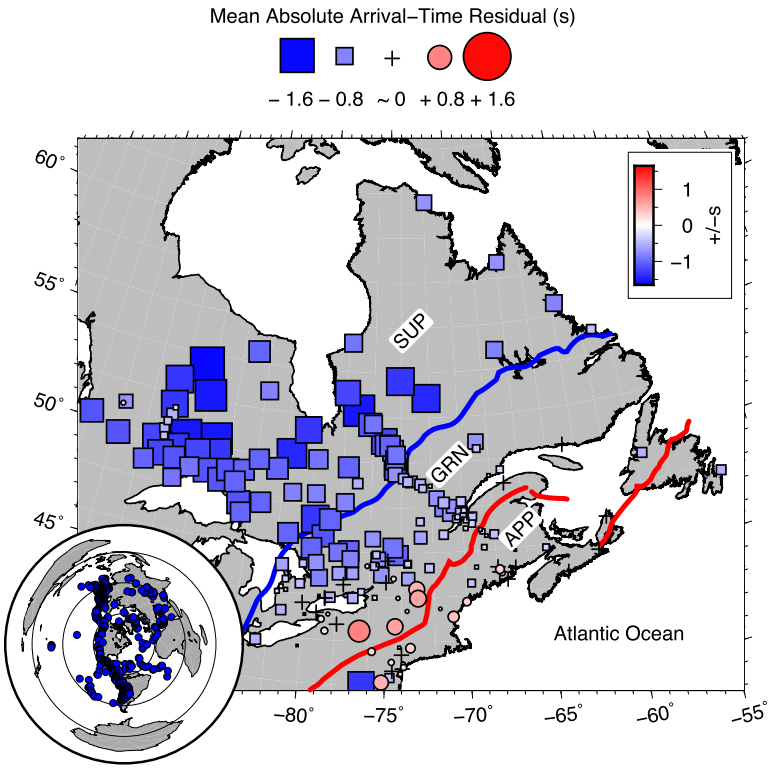


**Fig. 2.** Absolute arrival-time residuals for Eastern North America. Mean absolute arrival-time residuals for temporary seismic stations in southeast Canada derived from the AARM method (Boyce et al., 2017). Negative values represent early arrivals (fast) and positive values represent later arrivals (slow) with respect to ak135 (Kennett et al., 1995). The inset globe plots earthquakes contributing to this dataset.

May 2016. Typical interstation spacing is of the order of 70 km, which provides unprecedented spatial sampling for a continental seismic network. The phase path geometries, earthquakes, stations and direct-P residuals used in the inversion are shown in Figs. *S*1−*S*4.

### 2.2. Uniquely available datasets

To improve upon previous continental inversions for the U.S. (e.g., Schmandt and Lin, 2014; Burdick et al., 2017), we extend resolution northwards into the Canadian Shield regions by incorporating numerous smaller regional seismic networks (e.g., Frederiksen et al., 2013; Boyce et al., 2016). These include 9032 P arrivals from 238 earthquakes recorded in southeast Canada at 160 stations over the period 2007−2016 (Boyce et al., 2016, 2017), 3766 P arrivals from temporary seismic networks in the western Superior Province (Figs. S5 and S6) and 3599 P arrivals from the QM-III seismic network (Figs. S7 and S8), that traverses the interior of Québec to the Canadian Maritimes. Further details on analysis of these datasets can be found in Boyce et al. (2017).

These additional networks have, until now, only been used to report relative arrival-time residuals for use in regional tomographic inversions to study the local mantle wavespeed structure (e.g., Frederiksen et al., 2013; Boyce et al., 2016). Temporary seismic networks typically record at a lower signal-to-noise ratio than permanent observatory sites and thus it is a challenge to retrieve accurate timings for the first arrival of earthquake energy at such stations. Therefore relative arrival-time approaches remain widely used for temporary seismic networks. However, the recently-developed Absolute Arrival-time Recovery Method (AARM; Boyce et al., 2017) addresses this issue.

Teleseismic waveforms recorded at temporary seismic networks, for a single earthquake, are first filtered and aligned using a relative arrival-time technique (see Boyce et al., 2016). Time shifts determined from the filtered data are applied to the unfiltered data which are subsequently stacked using phase weighting (Boyce et al., 2017). An improved final stack is derived from weighting the contribution of the individual traces, according to signal-to-noise ratio or the cross correlation coefficient with the primary stack, upon which the first arrival is picked. Absolute arrival-times can therefore be recovered for the aligned waveforms using this earthquake-specific time correction. With this processing the Canadian temporary seismic network data (Fig. 2) can be included in an absolute wavespeed tomographic inversion.

Variation in relative arrival-time residuals typically results from wavespeed variations directly beneath a local seismic network, and as such first order variations may be easily seen (e.g., Boyce et al., 2016). Absolute arrival-time residuals however, document wavespeed variation along the entire ray path, from source to receiver. Individual residual measurements may therefore not solely represent upper mantle or lithospheric wavespeed structure beneath a seismic network. Fig. 2 shows mean absolute arrival-time residuals plotted for stations in southeast Canada derived from AARM (Boyce et al., 2017). Observable first-order patterns of wavespeed structure from beneath the Canadian networks are present because our dataset affords a good backazimuthal coverage of earthquakes (Fig. 2). By calculating the mean over the entire backazimuthal range at each station, the far-field component of the individual travel-time residuals is effectively downweighted. Global parameterization accounts for the far-field component of each residual within the subsequent inversion.

The Superior Province is dominated by negative residuals of greater than 1.0 s, with the earliest arrivals being recorded in the western Superior Province (Fig. 2). There is a marked decrease to negative residuals of less than 0.8 s, across the GF. The southeast Grenville and Appalachian Provinces are dominated by residuals of ∼0 s and low amplitude positive residuals (Fig. 2). The tectonically stable terranes of eastern Canada are typically dominated by high

seismic wavespeeds in global tomographic models (e.g., Li et al., 2008a; Priestley et al., 2019) consistent with these observations.

### 2.3. Inversion technique

Our tomographic inversion approach closely follows that of Li et al. (2008a) and Burdick et al. (2017). Rays are traced in the 1D reference model ak135 (Kennett et al., 1995), and are clustered to form weighted composite rays in regions of dense sampling (e.g., Li et al., 2008a). Initially, the model is parameterized globally on a regular grid with node spacing of 45 km in depth, 0.35° in latitude and longitude. Where ray sampling is poor, adjacent grid cells are combined up to a minimum ray count of 900 per cell (Fig. S9). An iterative, linearized, least squares inversion (LSQR) is used to solve for slowness with respect to ak135 (Kennett et al., 1995), and hypocenter mislocation parameters to minimize the following function:

$$\epsilon = \| wGm - wd \|^2 + \lambda_1 \| Lm \|^2 + \lambda_2 \| m \|^2 . \quad (1)$$

$G$ is the ray-theoretical sensitivity matrix, $m$ is the model (including both slowness and hypocenter mislocation parameters), $d$ is the data. $w$ controls the individual dataset weights; $L$ is a first-derivative smoothing operator. $\lambda_i$ control the weighting between each term relative to the first (i.e., model misfit). Regularization is required to overcome uneven sampling. In the least squares minimization of Equation (1), model roughness is controlled by the smoothing operator, $L$ and the value of $\lambda_1$. Model damping is controlled by the model norm weighted by the term $\lambda_2$. We determine regularization parameters using a trade-off curve approach (Fig. S10) for the globally parameterized model but make minor adjustments to account for the abundance of North American data (e.g., Golos et al., 2018). Although most of the LSQR convergence is reached quickly, we conduct 400 inversion iterations for all models. Our final model exhibits an RMS residual reduction of 47.2%. We account for crustal heterogeneity by making data-side corrections to the residuals ($d$), based on the model NACr14 (Tesauro et al., 2014). We propagate rays through the crustal model, calculate the component of each residual produced by the crustal model and remove this from the data vector ($d$) prior to the inversion. P-wave velocity anomalies are plotted as a percentage deviation from ak135 (Kennett et al., 1995).

### 2.4. Resolution assessment and dataset weighting

Spatial and temporal sampling varies dramatically between the dense USArray TA network (whose footprint terminates at ~48°N) and the Canadian networks. The abundance of TA data dominates the inversion in North America when datasets are weighted equally. We aim to balance the contributions of these networks in the inversion because we expect, to first order, similar seismic velocities for Precambrian lithospheric structures north and south of the U.S.-Canadian border (Schaeffer and Lebedev, 2014). Fig. 2 shows that arrivals may even be earlier further north in the Superior than at the U.S.-Canadian border. We construct a synthetic anomaly model of the Canadian Shield on the adaptively parameterized grid, centered at 100 km depth, beneath both the TA and temporary networks (Fig. 3). By using the forward problem to calculate arrival-time residuals through this synthetic structure, we invert these data and seek to recover the input model by balancing dataset weights. Amplitudes are best recovered with fewest artifacts when the smaller networks are weighted three times that of the EHB and TA datasets.

For a qualitative assessment of resolution for the dataset weighting criteria above, synthetic structure (Fig. 3, 4, $S11-S13$), and checkerboard resolution tests (Figs. $S14-S16$) are performed. We invert arrival-time residuals calculated for ray paths that are identical to those of the observed data, passing through a synthetic model of velocity perturbations, onto which gaussian noise of 0.2 s standard deviation is added.

Fig. 3 shows two synthetic tests motivated by structure recovered in the observed data inversion. Both synthetic models contain a low wavespeed anomaly ($-2.0\%\delta V_P$) in the western U.S. The shallow model (Fig. 3A, B) has a large high velocity structure centered in the upper lithosphere (100 km depth) that represents the high wavespeeds of the Archean and adjacent Grenville Province; the deeper model has a high velocity anomaly centered in the lower lithosphere (200 km depth), that represents the Mesoproterozoic and Archean domains west of the Grenville Province (Fig. 3C, D). The low velocity anomaly in the western U.S. is spatially well recovered in both models (amplitude recovery: ≥60% - shallow model, ≥75% - deep model: Fig. 3E, G). In the shallow model (Fig. 3E), the high velocity anomaly in the southern Canadian Grenville is spatially well recovered (amplitude recovery ≥40%). However, in the northeast Grenville and the northern Superior Province, amplitude recovery reduces (to ≤25%) and the lateral extent of anomalies is less tightly constrained due to sparser station coverage (Fig. 3E). Amplitude recovery in the deeper model is ≥50% in the eastern U.S. but <50% beneath the Superior Province in Canada (Fig. 3G). Again, lateral smearing increases northwards in the deeper model.

We invert for a Grenville-specific velocity anomaly structure that varies linearly with latitude, south-to-north, from $\delta V_P = -2.0\%$ to $\delta V_P = +2.0\%$. Fig. 4 shows structure confined to the upper 150 km; a range of upper mantle anomaly depth extents are shown in Figs. $S11-S13$. The low velocity anomaly in the southern Grenville/Ouachita Embayment is recovered with ≥50% amplitude, whilst the high velocities in Canada are recovered with ~25% amplitude that decreases towards Labrador in the northeast. Laterally the velocity anomaly structure is well constrained, specifically the location of the transition from low-to-high wavespeeds around the U.S.-Canadian border (Fig. 4E, H).

Finally we perform checkerboard tests using 5° and 10° anomalies. Alternating regions of $\delta V_P = \pm 2\%$ are input to estimate variations in spatial recovery (Figs. S14A, B and S15A, B). Beneath the continental U.S., recovery amplitudes across both checkerboard tests are ~40% at 200 km depth and increase to ≥50% at 500−800 km depth (Figs. S14F-H and S15F-H). At 200 km depth in northeastern Canada (Figs. S14F and S15F), amplitude recovery of the checkerboard anomalies is <25% of input amplitudes as a result of sparse station density. However, in eastern Canada, particularly when using larger 10° checkerboards (S15F) the lateral extent of input velocity anomalies is well recovered as a direct result of including additional Canadian network data. Next we aim to quantitatively assess the extent of smearing and the minimum resolvable scale within BBNAP19.

By overlaying the recovered synthetic resolution tests upon the input anomalies from Figs. 3 and 4, in Fig. S16 we can visually estimate the amount of lateral smearing present at the Grenville and Appalachian fronts in the lithosphere. In the U.S. Grenville, lateral smearing of input anomalies appears to be <50 km. In the Canadian Grenville, lateral smearing appears to be ~50 km, increasing to ≥100 km in Labrador in the far northeast. Whilst vertical smearing is unavoidable in body wave tomography, the broad input anomalies (Fig. 3B, D) are reasonably well constrained in depth by the recovered amplitudes of ≥40% beneath the USArray TA stations (Fig. 3F, H). The shallow synthetic resolution tests (Figs. 3B, F, S11 and S12) may suffer vertical smearing of >100 km whilst the deeper synthetic tests (Figs. 3D, H, 4 and S13) display vertical smearing of ~100 km. Significant vertical smearing (>100 km) is only seen at the edge of the checkerboard models (Figs. S14C-E and S15C-E).

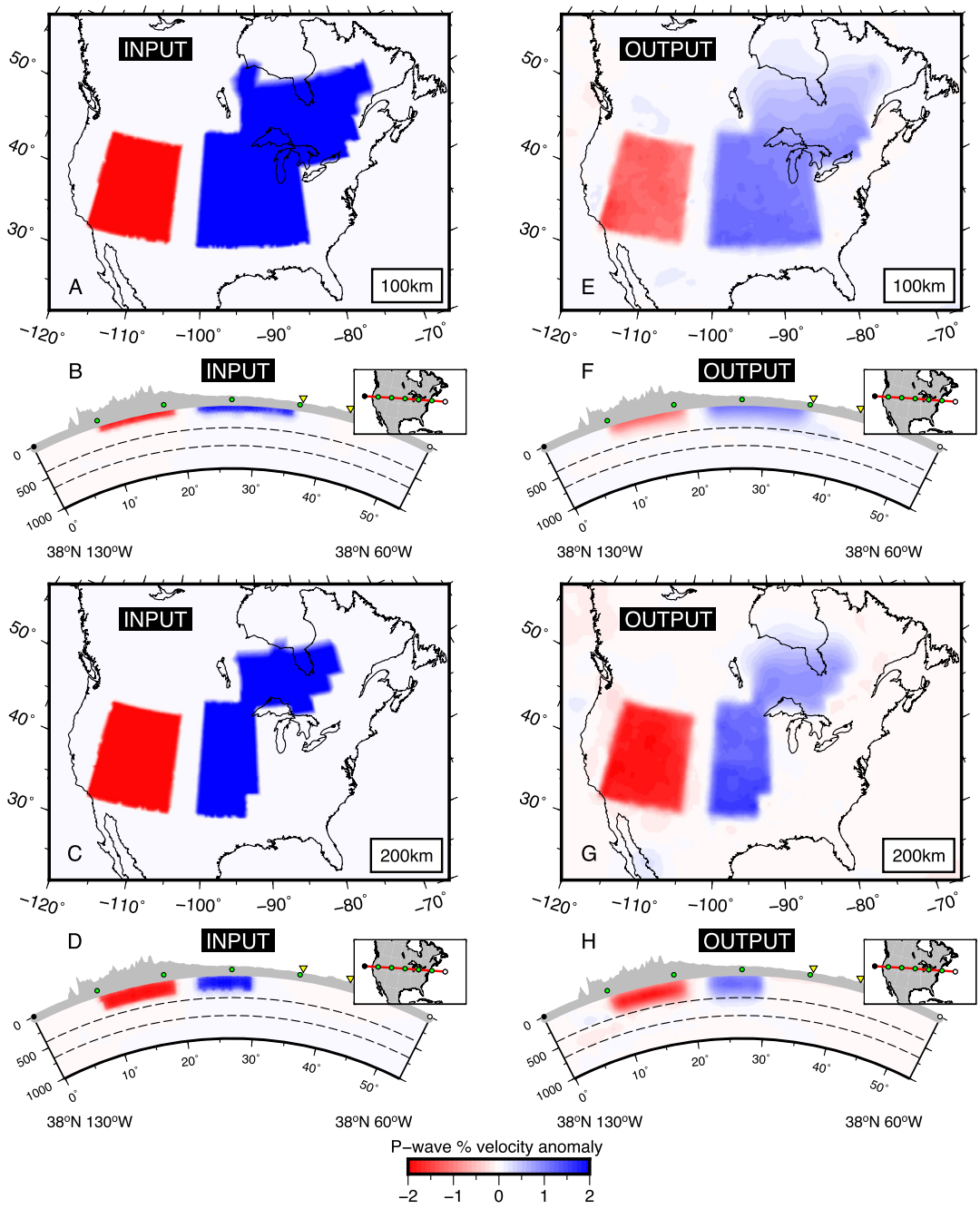


**Fig. 3.** Synthetic resolution tests for North America. Structural resolution tests for $\delta V_P = \pm 2.0\%$ input velocity anomalies centered at 100 km (A, B) and 200 km (C, D). A-D are the input models, E-H, are the recovered models.

By inverting for checkerboard anomalies of increasing size using the methodology outlined above (1.5−10°; Fig. S16), we investigate the minimum resolvable distinct velocity anomaly in the Grenville Province. In laterally well resolved regions, we consider the minimum resolvable scale to be half the width of the input checkers. At 35°N in the U.S. Grenville, 2° velocity anomalies are recovered, which equates to a minimum resolvable scale of ~90 km, comparable to the average station spacing of the USArray TA (~70 km). In eastern Canada, 5−7.5° input checkers are recovered except in northeastern Labrador and the northern Superior Province where only input checkers ≥10° are resolved. In the Canadian Grenville (at ~50°N), we estimate a minimum resolvable scale of ~175−260 km. This increase largely reflects the increase in station spacing in Canada. The width of the Grenville varies from 150−700 km south-to-north. Based on the tests outlined above, long wavelength (≫1000 km) wavespeed observations within the Grenville upper mantle (≤300 km depth) and abrupt lateral wavespeed boundaries, particularly in the U.S., are robust features of BBNAP19.

## 3. New P-wave tomography model for North America

### 3.1. Features of the new P-wave tomography model for North America

At the continent scale, BBNAP19 shows the North American shallow mantle velocity structure (100−250 km depth) to be dominated by pervasive low velocities ($\delta V_P \leq -0.75\%$) in the west, transitioning to high velocities ($\delta V_P \geq 0.5\%$) in the Proterozoic central-

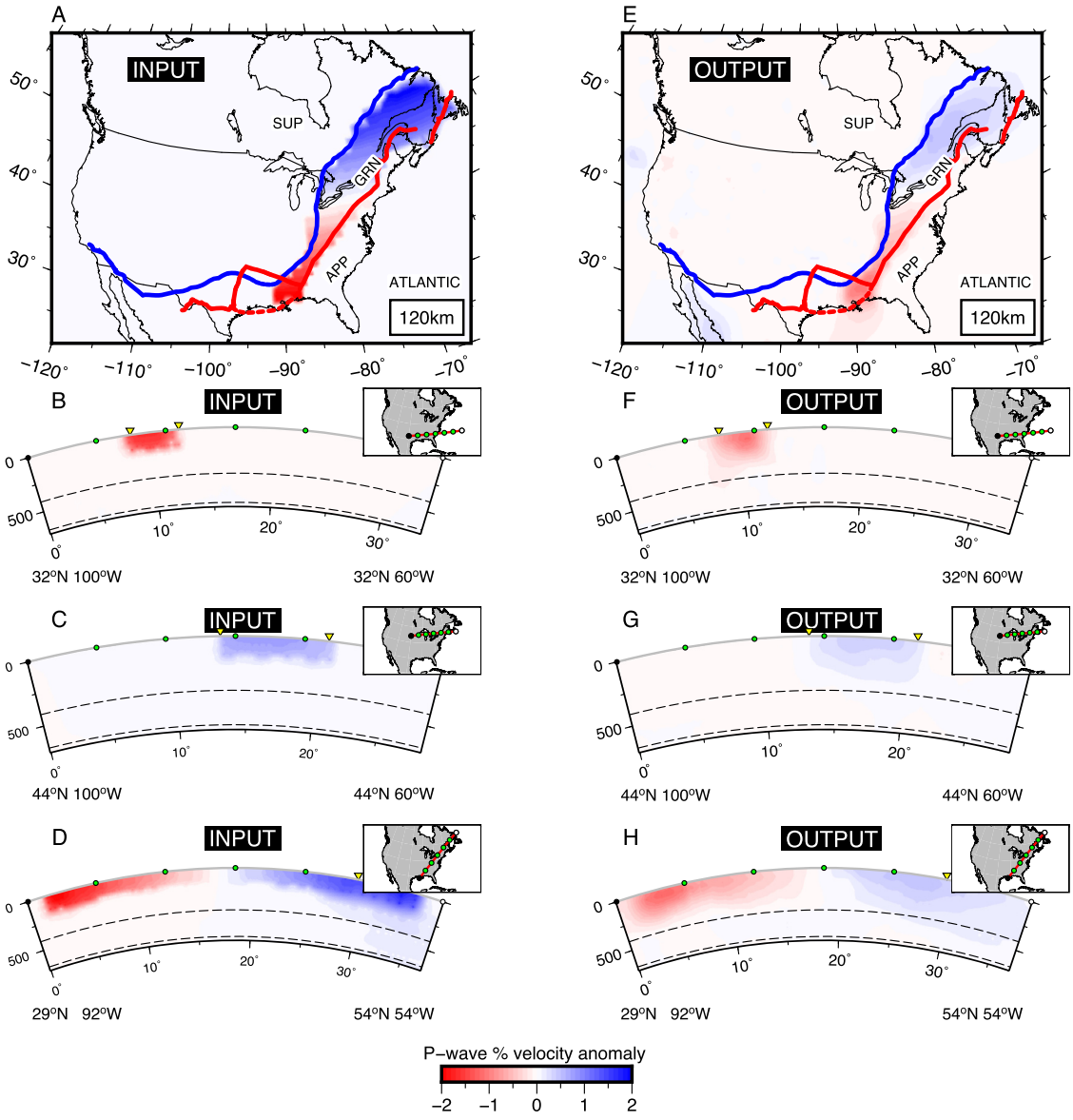


**Fig. 4.** 150 km depth Grenville specific resolution test. Grenville specific resolution test showing recovery of a synthetic velocity anomaly linearly varying from $\delta V_P = -2.0\%$ to $\delta V_P = +2.0\%$ south-to-north in the Grenville Province at $\leq$150 km depth. A-D show the input velocity model, E shows the output model at 120 km depth, F-H show cross sections through the output model at 32°N, 44°N and parallel to the Grenville Province.

eastern regions (Figs. 5 and 6). The eastern coastal Appalachian terranes show largely average-to-low velocities ($-0.4\% \leq \delta V_P \leq 0.2\%$). Two strong localized low velocity anomalies ($\delta V_P \leq -1.0\%$) exist in the Appalachians (Fig. 5). The northern Appalachian anomaly (NAA) may extend to depths of 250 km whilst the central Appalachian anomaly (CAA) is restricted to shallower depths (see cross sections at 36°N and 32°N, respectively in Fig. 6). In the south, the Ouachita Embayment is characterized by average velocities ($-0.2\% \leq \delta V_P \leq 0.2\%$) from 100–250 km depth (Fig. 5).

### 3.2. Eastern North American lithosphere

At depths of 100–150 km in the north-eastern continental region (≥42°N), high velocities ($\delta V_P \geq 0.5\%$) exist throughout the Superior Province and extend eastward into the Grenville Province (Fig. 5), albeit slightly lower in amplitude. In the southern U.S. Mid-Continent (≤42°N), the high velocities of the North American shield extend from the N-S trending boundary at ∼100°W terminating abruptly coincident with the inferred location of the GF (Fig. 5). The U.S. Grenville Province is dominated by low velocities ($-0.5\% \leq \delta V_P \leq 0\%$) in contrast to the continental interior. These shallow mantle seismic velocity boundaries are well resolved in BBNAP19 (Figs. 3, 4 and $S11-S16$).

At depths of 200–250 km beneath the Canadian Grenville, low amplitude high velocities ($\delta V_P \leq 0.3\%$) extend from the Superior Province eastwards across the GF (Figs. 5 and 6). In the U.S., the highest velocities are again restricted to west of the GF but the Grenville Province is dominated by approximately average velocities ($\delta V_P \sim 0\%$). In the far south, at the Grenville's narrowest point (∼32°N, 86°W), the high velocities of the Proterozoic central-eastern do extend across both the GF and the AF at 100–250 km depth, but amplitudes decrease with depth. At model depths likely below the base of the lithosphere (≥300 km), high wavespeed anomalies in Canada appear to be vertically smeared from shallower depths due to sparser station coverage. The U.S. is largely dominated by broad low-amplitude velocity anomalies ($-0.3\% \leq \delta V_P \leq 0.3\%$), again perhaps the result of some vertical smearing.

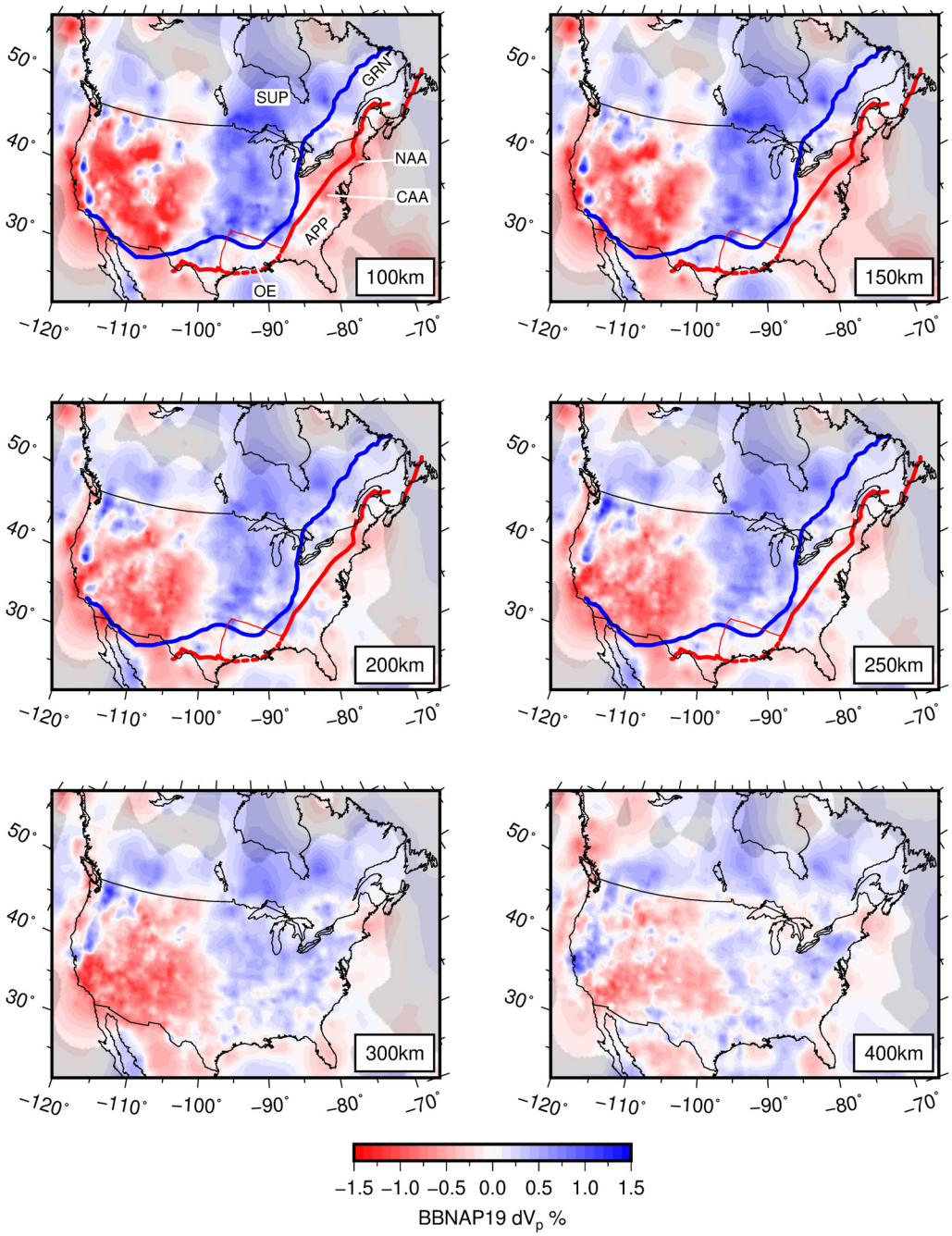


**Fig. 5.** Tomographic model for North American upper mantle. Upper mantle results from the Boyce-Bastow North America P-wave model 2019 (BBNAP19) plotted as a percentage deviation from ak135. Grey regions are poorly recovered by the 10° checkerboard resolution test (Fig. S15). Tectonic boundaries are plotted for reference (Fig. 1). NAA - northern Appalachian anomaly, CAA - central Appalachian anomaly.

East-west striking cross-sections at 42−38°N across North America (Fig. 6B-D) also show the high velocities to extend from the Superior into the Canadian Grenville Province to ∼250 km depth. However in the U.S., at 36−30°N (Fig. 6E-H), an abrupt wavespeed boundary coincident with the GF is apparent at ≤200 km depth. High wavespeeds also appear to extend eastwards from the Precambrian interior at ≤400 km depth.

Even when considering vertical ray-path smearing (Figs. 3 and 4), BBNAP19 indicates that there is a significant difference in P-wave velocities along strike in the upper mantle of the Grenville orogen (at least ≤150 km depth; Figs. 5 and 6). The wavespeed difference (∼1%) between the north and south Grenville is shown more strikingly in Fig. 7 in which the average velocity of eastern North America (+0.13%$\delta V_P$ at 100 km depth) is subtracted before plotting. The northern Grenville exhibits regions of higher than average velocities whilst the south is lower, bounded clearly at its western edge by the Grenville front. This first order observation suggests the Grenville orogen is heterogeneous along strike in the mantle.

## 4. Discussion

### 4.1. Causes of seismic heterogeneity

By incorporating numerous seismic networks from eastern Canada into a continental P-wave model for North America, the

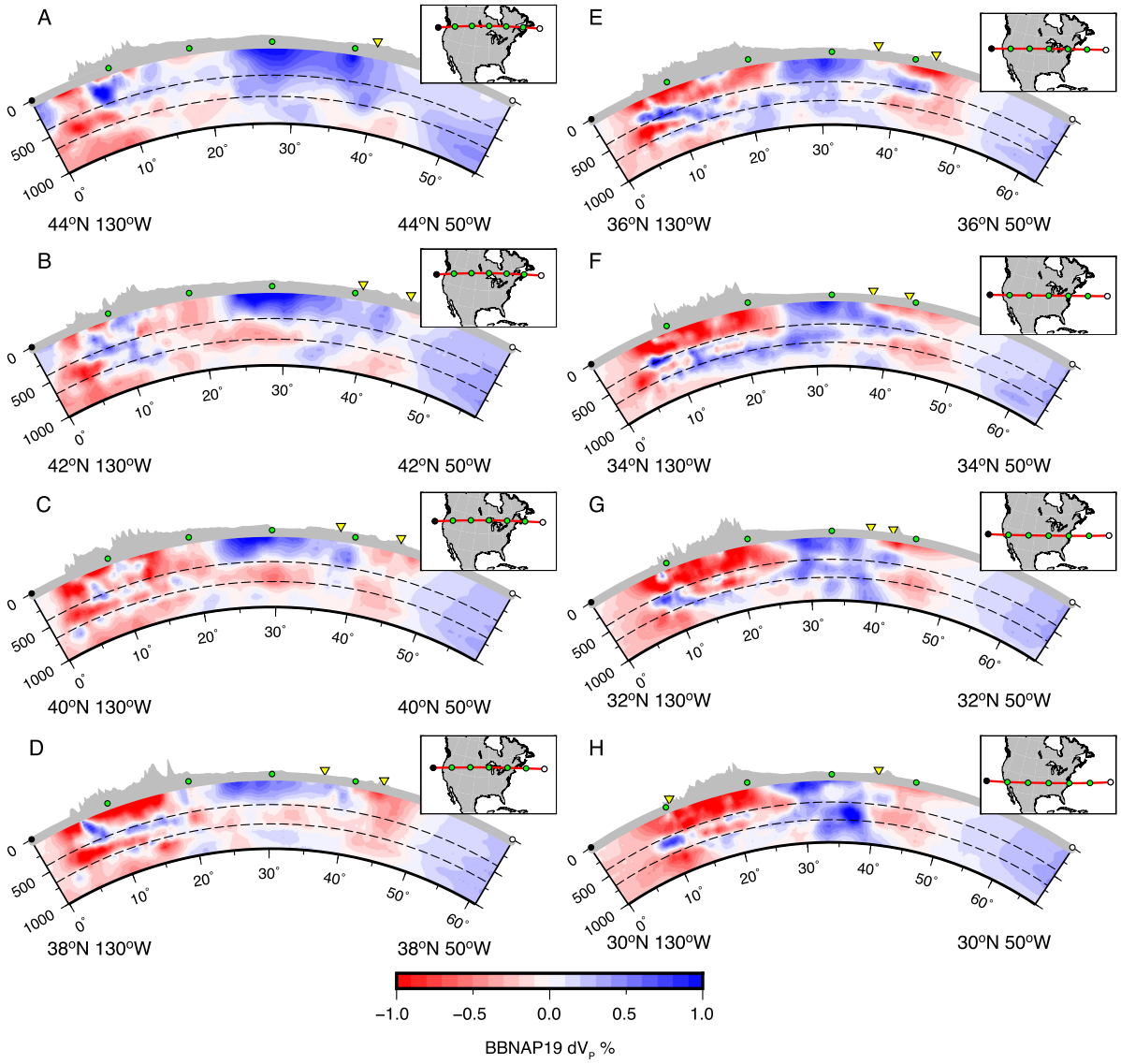


**Fig. 6.** Cross sections through tomographic model for North America. Cross sections through BBNAP19, plotted as a percentage deviation from ak135. Cross sections show exaggerated topography in grey and location of GF and AF tectonic boundaries at the surface as yellow triangles (Fig. 1).

data used in BBNAP19 can resolve heterogeneity along the entire Grenville Province (Figs. 5-7). Previous studies have focused on smaller regions using relative arrival-times (Biryol et al., 2016; Boyce et al., 2016) or lack resolution in the Canadian Grenville (Li et al., 2008a; Schmandt and Lin, 2014; Burdick et al., 2017). A striking observation in BBNAP19 is the apparent decrease in P-wavespeeds within the Grenville from north-to-south (Figs. 5-7), unseen in recent shear wave models (Fig. 8; Schaeffer and Lebedev, 2014; Schmandt and Lin, 2014; Pollitz and Mooney, 2016; Priestley et al., 2019). These models generally show high shear velocities throughout the entire Grenville, gradually decreasing eastwards towards the coast.

Presently, lithospheric thickness does not vary greatly along the entire Grenville Province (Fig. 1; Priestley et al., 2019). The preserved Grenville mantle lithosphere has remained largely tectonically quiescent since formation in the Proterozoic, having only been affected by localized Great Meteor hotspot tectonism (at ca. 190−110 Ma; Heaman and Kjarsgaard, 2000), although to a lesser extent than the adjacent Appalachians (Boyce et al., 2016).

Rift basin development in the Mid-Continent (1.2−1.1 Ga) and southeastern U.S. (620−535 Ma) was not followed by rifting of the Laurentian continent (Whitmeyer and Karlstrom, 2007; Li et al., 2008b). Seismic signatures of rift basin formation are restricted to the crust and very shallow mantle (Pollitz and Mooney, 2016) and as such is not seen in the mantle lithosphere (∼100−250 km depth) of BBNAP19 (Figs. 5 and 7). Replacement of depleted continental lithosphere with younger asthenospheric material within these failed rift arms would probably result in a similar, largely symmetrical effect in $V_S$ and $V_P$, about the rift segment axis.

Gravitational destabilization (e.g., Harig et al., 2010) or convective removal of mantle lithosphere (e.g., Bao et al., 2014), resulting in the formation of younger, less depleted lithosphere beneath the Grenville Province is expected to produce similar signatures in $V_S$ and $V_P$ images, whether ongoing today (e.g., Biryol et al., 2016) or relatively soon after Grenville formation. Present-day lithospheric removal (Biryol et al., 2016) would produce several other observables (Harig et al., 2010) pervasive throughout the southern Grenville, but evidence for widespread volcanism (Mazza et al., 2014), uplift (Liu, 2015) and significant lithospheric thinning (Priestley et al., 2019) is lacking. Further, systematic variation in age, compositional or spatial distribution of post-collisional gran-

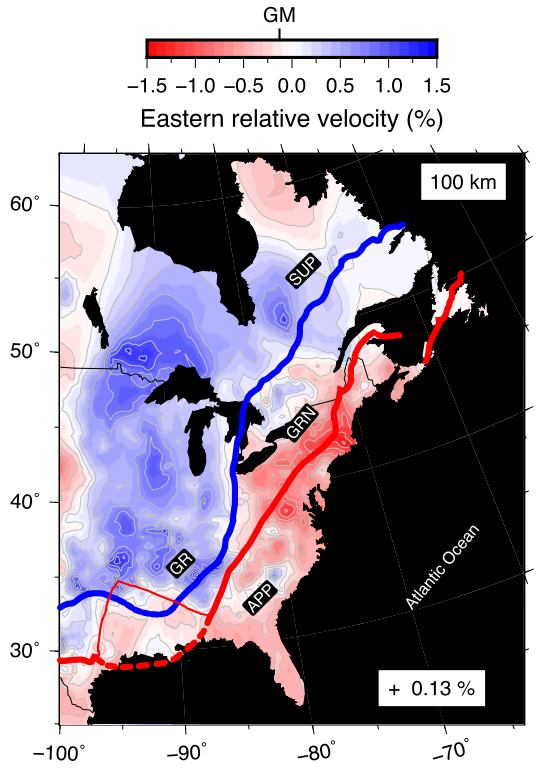


**Fig. 7.** 100 km depth "relative velocity" snapshot of BBNAP19. BBNAP19 tomographic image of eastern North America in which velocity is plotted as a percentage deviation from the regional average ($+0.13\%\delta V_P$ at 100 km depth) within the plotted area (105–50°W, 25–65°N). The position of the global mean velocity is indicated (GM). Of particular note is the change from relatively high velocities in the northern Grenville to low velocities in the southern Grenville, compared to the regional average.

ites (Harig et al., 2010) would be required to support a hypothesis of variable lithospheric removal along strike since Grenville formation, but no such evidence exists (Davidson, 1995; Whitmeyer and Karlstrom, 2007). We therefore seek an alternative explanation for the north-south divide in lithospheric P-wavespeeds that does not result in a change in $V_S$.

Within the continents, temperature is the main control on seismic velocity (Schutt and Lesher, 2006; McKenzie and Priestley, 2008). Thermal diffusion, which occurs on timescales of ∼50 Myr for small regional lithospheric anomalies (e.g., Eaton and Frederiksen, 2007), likely prevents temperature variations giving rise to abrupt wavespeed boundaries within Grenville orogen (Figs. 5-7; Boyce et al., 2016). Further, anomalously warm, wet or partially molten mantle leads to a stronger reduction in $V_S$ than $V_P$ (Wagner et al., 2008), an antithetical result to the one we require. $V_P$ is only very weakly sensitive to lithospheric melt depletion (Schutt and Lesher, 2006), the compositional signature derived from mantle keel formation (Jordan, 1978; Hawkesworth et al., 1990). However metasomatism, more specifically, the addition of silica to olivine, results in lithospheric enrichment in orthopyroxene by water-rock/melt-rock interaction at marginal subduction zones (Kelemen et al., 1998; Wagner et al., 2008). This can decrease $V_P$ by more than 1% within depleted mantle lithosphere, with little effect on $V_S$ and density (Schutt and Lesher, 2010). Consequently, the low $V_P/V_S$ observations in the overriding lithosphere (of up to Grenvillian age ∼1.1 Ga) above the present-day Peru-Chile subduction zone, are attributed to orthopyroxene enrichment (Wagner et al., 2008). Abrupt $V_P$ variations imaged in BBNAP19 (Figs. 5-7) may, therefore, be best explained by a Grenvillian metasomatic process that modified the lithospheric mantle composition.

### 4.2. A north-south transition in the Grenville orogen

Our observations of along strike variation in $V_P$ accompanied by little variation in $V_S$ (Fig. 8) within the Grenville orogen can be explained by varying resistance to metasomatic alteration during protracted subduction along the Laurentian margin (≥300 Myr) that preceded terminal collision (Rivers, 2009). The Canadian Grenville, prior to 1.3 Ga, was likely underlain by depleted (Jordan, 1978; Hawkesworth et al., 1990), viscous (Sleep, 2003), refractory Archean Superior lithosphere at time of collision (Ludden and Hynes, 2000; Whitmeyer and Karlstrom, 2007). Because only a small decrease in $V_P$ is seen within the upper lithosphere in BBNAP19 across the GF, modification of the refractory Canadian Grenville mantle lithosphere through metasomatism, as suggested by previous studies (Chiarenzelli et al., 2010; Boyce et al., 2016), may have been weak (Griffin et al., 2004). To modify depleted cratonic lithosphere to a much greater extent would require metasomatism to a greater degree than has been observed (Wenker and Beaumont, 2018).

In contrast, in the U.S. the GF cross-cuts the young (≤250 Myr old at the time of collision), less refractory (Hawkesworth et al., 1990), Granite-Rhyolite terrane (Fig. 1; Whitmeyer and Karlstrom, 2007) and is accompanied by a significant (∼1%) decrease in $V_P$ within the upper lithosphere (Figs. 5 and 6). Modification of the mantle lithosphere here appears to be strong, as suggested by analysis of garnet xenocryst samples from kimberlites within the U.S. Grenville (Griffin et al., 2004). Young, less refractory lithosphere is inherently more susceptible to strong modification (Wenker and Beaumont, 2018). The strong $V_P$ reduction across the GF in the U.S. may therefore be best explained by strong orthopyroxene enrichment (Wagner et al., 2008; Schutt and Lesher, 2010) of the mantle above the Grenvillian subduction zone. Lithospheric weakening could also be enhanced by extensive slab dehydration (Liao et al., 2017) throughout the protracted subduction phase (Rivers, 2009). In this interpretation, the coeval post-collisional granites found throughout the Grenville Province (Davidson, 1995; Whitmeyer and Karlstrom, 2007) are produced by internal heating of the thickened crust during protracted terminal continental collision (Jackson et al., 2008). Subsequently, these rocks are largely removed by erosion leaving dry granulite facies rocks behind (Jackson et al., 2008), as is observed throughout the exposed Canadian Grenville (Davidson, 1995; Rivers, 1997).

The downward increasing wavespeed anomaly in the U.S. Grenville (100−150 km $-0.5\% \leq \delta V_P \leq 0\%$ to 200−250 km $\delta V_P \sim 0\%$) may imply that metasomatism is strongest within the shallow lithospheric mantle and weaker below. This has been suggested for the thick Archean cratonic regions of the Slave and Kaapvaal craton for example (Eeken et al., 2018). Due to the juvenile state of the Granite-Rhyolite terrane at the time of the Grenville (and presumably thinner lithosphere than observed at present) a more likely explanation of the increase in wavespeed with depth would be that the mantle lithospheric keel stabilized at a later time and as such was less/not affected by metasomatic processes in the Grenville orogeny. This interpretation is supported by two-stage keel formation proposed by Yuan and Romanowicz (2010) for North America and Darbyshire et al. (2013) for the Proterozoic Trans-Hudson orogen within the Canadian shield. Following these ideas, below we speculate on the implications for the preservation of the Grenville Province and Proterozoic lithosphere.

### 4.3. Preservation of the Grenville orogen

Thick, strong lithosphere is difficult to shorten (McKenzie and Priestley, 2008). As such, mountain belts form at the margins; the weaker in-coming material in the collision is forced over the top (Chen et al., 2017). This is observed in Tibet (Jackson et al., 2008)

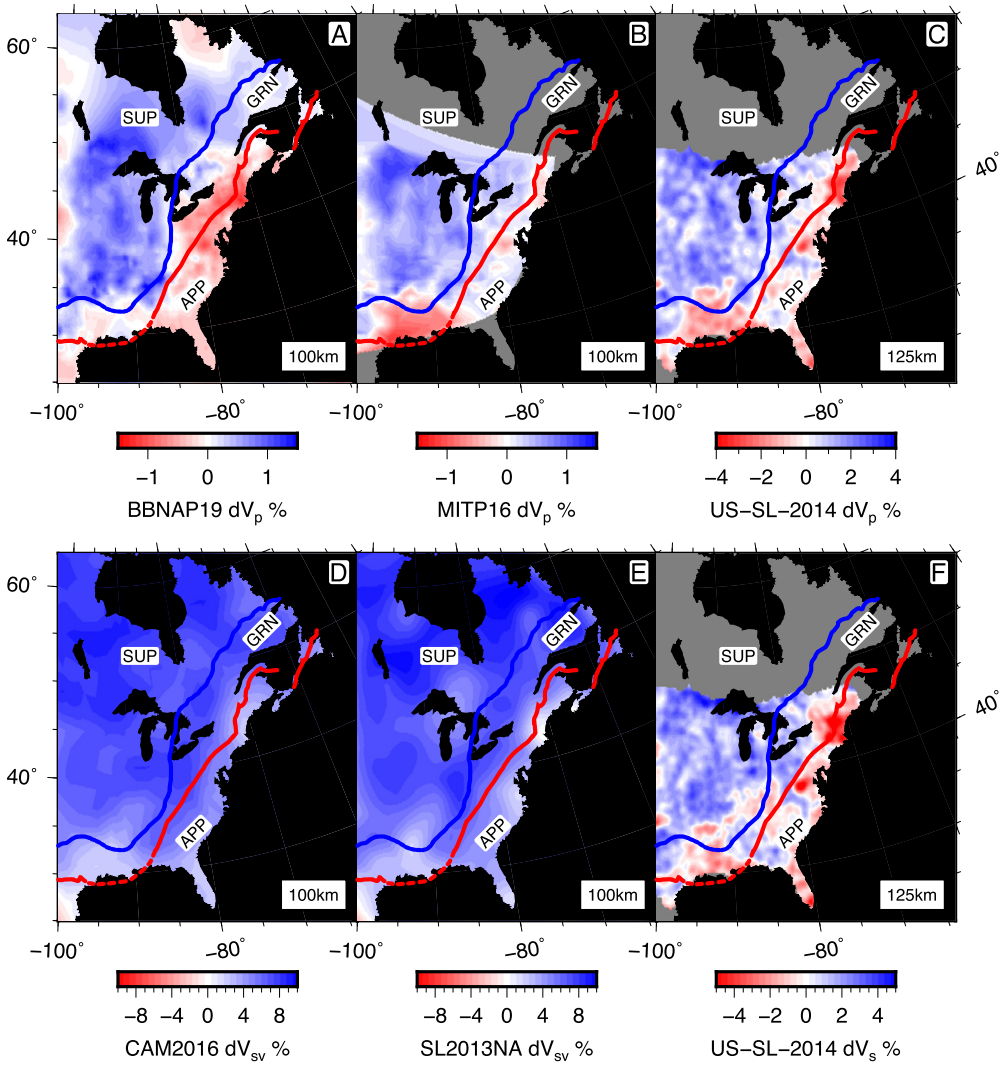


**Fig. 8.** Comparison of BBNAP19 with P- and S-wave models. Comparison of (A) BBNAP19 with (B) MITP16 (Burdick et al., 2017), (C) US-SL-2014-P (Schmandt and Lin, 2014), (D) CAM2016Vsv (Priestley et al., 2019), (E) SL2013NA (Schaeffer and Lebedev, 2014) and (F) US-SL-2014-S (Schmandt and Lin, 2014), at 100 – 125 km depth. BBNAP19 is plotted with the same color scale as Fig. 5. Grey regions within the continents are outside the parameterized model space.

and the Canadian Grenville orogen in which Proterozoic material was thrust above Archean Superior lithosphere (Ludden and Hynes, 2000). In contrast, significantly modified (and probably weaker) lithosphere, as is present in the south, is easily shortened and leads to the formation of a wide orogenic plateau (Chen et al., 2017), but subsequently will also undergo lithospheric collapse and thin more easily. When collisional belts undergo extension, some extension may occur in the shallow crust, often in an orogen-parallel sense (Rivers, 2012), but lithospheric-scale deformation is concentrated at the edge of the underthrust thick lithosphere (Sloan et al., 2011), not the overthrust orogenic front seen at the surface. Deep (>15 km) crustal earthquakes in the northern Grenville concentrate towards the Appalachian Front, away from the GF, but occur throughout the southern Grenville at shallow depths (Fig. 1). This is consistent with the presence of strong (and consequently less seismogenic) lithosphere beneath the interior Canadian Grenville compared to that further south.

This offers a simple explanation for a broad northern Grenville and narrow southern Grenville preserved today (~700–500 km compared to ~500–150 km; Fig. 1). Rifting of Laurentia, and subsequent deformation during the Appalachian orogeny concentrated ≥500 km oceanward of the northern GF, at the edge of the thick, depleted lithosphere. In contrast, either much of the southern, perhaps thinner, Grenville was rifted away or Appalachian overprinting was greater in the south because strong, depleted lithosphere did not exist there.

Because Mid-Continent rifting is inadequate to explain the abrupt $V_P$ decrease in the shallow lithosphere co-located with the gravity anomalies of Stein et al. (2017), a further implication of our observations (Figs. 5-7) and subsequent interpretation is that the Grenville Front almost certainly is preserved in the U.S. Grenvillian processes seemingly did affect the lithosphere there despite having gone largely undetected seismically, previously (e.g., Schmandt and Lin, 2014; Burdick et al., 2017).

### 4.4. Preservation of Proterozoic lithosphere

The Proterozoic Labradorian and Mazatzal terranes, affected by Grenvillian orogenic processes in the north, were likely underthrust by Archean remnants (Ludden and Hynes, 2000). In the south, the juvenile (≤250 Myr old) and probably thin Granite-Rhyolite lithosphere was likely non-buoyant and non-refractory (Hawkesworth et al., 1990) at the time of the Grenville collision, thus rendering it more susceptible to metasomatic modification and subsequent thickening and stretching. To the west of the GF, the Yavapai, the Mazatzal and western Granite-Rhyolite terranes were not affected by Grenvillian processes. Expressions of tectonic

processes within these terranes (such as Mid-Continent rifting) are limited to the crust and very shallow mantle throughout the Proterozoic (Whitmeyer and Karlstrom, 2007; Pollitz and Mooney, 2016). Therefore, these terranes are likely to have thermally stabilized since their formation, perhaps leading to the formation of their thick mantle keel during the Proterozoic (e.g., Yuan and Romanowicz, 2010). This indicates that Proterozoic lithosphere may only be long-lived in its original unmodified state when it is isolated from lithospheric-scale tectonic processes (e.g., west of the GF) or Proterozoic-aged crust is underthrust by more depleted (perhaps Archean) lithosphere, as is observed in the northern Grenville (Ludden and Hynes, 2000). Juvenile Proterozoic lithosphere has been observed to be more enriched (Hawkesworth et al., 1990; Griffin et al., 2004) than that of Paleoproterozoic and Archean regions. In regions such as the southern Grenville, orthopyroxene enrichment could account for these observations and thus render the juvenile enriched Proterozoic Grenville lithosphere more similar to present-day lithosphere than commonly thought (Hawkesworth et al., 1990). This would offer an explanation for the similar $V_P$ observed between the modified Grenville and adjacent Appalachian terranes in the thick lithosphere of the eastern U.S.

Eaton and Perry (2013) showed that Proterozoic cratonic keels obtain their long-lived buoyancy after ∼1 Gyr. The modified Granite-Rhyolite terrane was less than 250 Myr old at the time of the Grenville collision. After 250 Myr, a Proterozoic keel's initial interior buoyancy decays by greater than 60% towards its long-lived state from either a hot or cold starting model (Eaton and Perry, 2013). Our observations suggest at least 250 Myr is required to inhibit modification of Proterozoic lithosphere, perhaps because a shielding thermal boundary layer component of the mantle keel had yet to form. This is consistent with the approximate thermal time constant of the continental lithosphere (∼250 Myr; McKenzie and Priestley, 2016).

## 5. Conclusions

We present a new model of eastern North American mantle P-wave structure using data from temporary seismograph networks from the Canadian core of Laurentia to supplement permanent and continental-scale deployments. Specifically we examine the deep seismic structure of the ∼1.3−1.0 Ga Grenville orogen, whose longevity and present-day setting, far from any active plate boundary, make it an ideal locale to study the Precambrian modification processes at the margin of stable lithosphere. Our model (BBNAP19) provides important insight into the evolution of the proto-North American eastern margin because P-waves are sensitive to fluid/melt-derived orthopyroxene enrichment of depleted continental lithosphere after formation, whilst S-waves are not. BBNAP19 shows high seismic wavespeeds extend from the Archean Superior craton into the Proterozoic Grenville terranes in the upper mantle (≤250 km depth) beneath eastern Canada. High wavespeeds are restricted to west of the Grenville front particularly in the upper lithosphere (≤150 km depth) in the U.S.

We propose that subduction derived metasomatism beneath the continental margin during the Grenville collision modified the overlying lithosphere to reduce seismic P-wave velocities with respect to the unmodified interior. In the north, the thick, refractory, Archean lithosphere was able to resist strong modification during subduction and subsequent orogenesis, whilst the younger lithosphere in the south was strongly modified by metasomatism. The lithospheric modification of the Granite-Rhyolite terrane during the Grenville orogeny suggests that at least 250 Myr must pass for Proterozoic continental lithosphere to stabilize and develop resistance to modification, perhaps through development of a thick mantle keel. Our work shows the importance of constraining absolute compressional velocities to complement shear velocities beneath regions of Precambrian lithosphere to better understand craton margin evolution.

## Data and resources

Phase arrivals from USArray are available to the community as CSS monthly files from the ANF http://anf.ucsd.edu/tools/events/download.php. Arrivals from the EHB Bulletin are available at http://www.isc.ac.uk/ehbbulletin/. Waveform data for southeast Canada and northeast U.S. are available through the Canadian National Data Centre and IRIS Data Management center. AARM-derived absolute arrival-time residuals and a digital model file will be made available through http://ds.iris.edu/ds/products/emc/ or by contacting the corresponding author (email: ab2568@cam.ac.uk).

## Funding

A.B. was funded by the Natural Environment Research Council Doctoral Training Partnership: Science and Solutions for a Changing Planet - Grant number NE/L002515/1 and subsequently NE/R010862/1 from PI Cottaar in Cambridge. I.B. acknowledges support from the Leverhulme Trust (grant RPG-2013-332). S.R. was supported by Career Integration Grant 321871-GLImER from the FP7 Marie Curie Actions of the European Commission and by the Research Council of Norway FRINATEK programme through SWaMMIS project 231354. This work was also supported by a Royal Society International Exchanges grant IE160131.

Our funding sources had no involvement with the design, processing, analysis, interpretation, manuscript preparation or article submission decision.

## Contributors

A.B. Designed study (and initiated collaboration), conducted analysis, interpreted data, prepared initial manuscript, revised/drafted manuscript critically, approved final version. I.B. Designed study (and initiated collaboration), interpreted data, revised/drafted manuscript critically, approved final version. E.G. Conducted collaborative study design, aided AB in conducting analysis, revised/drafted manuscript critically, approved final version. S.R. Conducted collaborative study design, interpreted data, revised/drafted manuscript critically, approved final version. S.B. Conducted collaborative study design, aided AB in conducting analysis, revised/drafted manuscript critically, approved final version. R.H. Conducted collaborative study design, interpreted data, revised/drafted manuscript critically, approved final version.

## Acknowledgements

We thank Andrew Hynes for his thoughtful discussion of this manuscript throughout its preparation. We thank the editor and two reviewers for their helpful clarifications.

## Appendix A. Supplementary material

Supplementary material related to this article can be found online at https://doi.org/10.1016/j.epsl.2019.115763.

## References

Bao, X., Eaton, D.W., Guest, B., 2014. Plateau uplift in western Canada caused by lithospheric delamination along a craton edge. Nat. Geosci. 7, 830–833. https://doi.org/10.1038/ngeo2270.

Biryol, B.C., Wagner, L.S., Fischer, K.M., Hawman, R.B., 2016. Relationship between observed upper mantle structures and recent tectonic activity across the southeastern United States. J. Geophys. Res. 121, 3393–3414. https://doi.org/10.1002/2015JB012698.

Boyce, A., Bastow, I.D., Darbyshire, F.A., Ellwood, A.G., Gilligan, A., Levin, V., Menke, W., 2016. Subduction beneath Laurentia modified the eastern North American cratonic edge: evidence from P wave and S wave tomography. J. Geophys. Res. 121, 5013–5030. https://doi.org/10.1002/2016JB012838.

Boyce, A., Bastow, I.D., Rondenay, S., Van der Hilst, R.D., 2017. From relative to absolute teleseismic travel-times: the Absolute Arrival-time Recovery Method (AARM). Bull. Seismol. Soc. Am. 107, 2511–2520. https://doi.org/10.1785/0120170021.

Burdick, S., Vernon, F.L., Martynov, V., Eakins, J., Cox, T., Tytell, J., Mulder, T., White, M.C., Astiz, L., Pavlis, G.L., Van der Hilst, R.D., 2017. Model update May 2016: upper-mantle heterogeneity beneath North America from travel-time tomography with global and USArray data. Seismol. Res. Lett. 88, 319–325. https://doi.org/10.1785/0220160186.

Card, K., 1990. A review of the Superior Province of the Canadian Shield, a product of Archean accretion. Precambrian Res. 48. https://doi.org/10.1016/0301-9268(90)90059-y.

Chen, L., Capitanio, F.A., Liu, L., Gerya, T.V., 2017. Crustal rheology controls on the Tibetan plateau formation during India-Asia convergence. Nat. Commun. 8, 15992. https://doi.org/10.1038/ncomms15992.

Chiarenzelli, J., Lupulescu, M., Cousens, B., Thern, E., Coffin, L., Regan, S., 2010. Enriched Grenvillian lithospheric mantle as a consequence of long-lived subduction beneath Laurentia. Geology 38, 151–154. https://doi.org/10.1130/G30342.1.

Currie, C.A., Wijk, J.v., 2016. How craton margins are preserved: insights from geodynamic models. J. Geodyn. 100, 144–158. https://doi.org/10.1016/j.jog.2016.03.015.

Darbyshire, F., Bastow, I., Petrescu, L., Gilligan, A., Thompson, D., 2017. A tale of two orogens: crustal processes in the Proterozoic Trans-Hudson and Grenville Orogens, eastern Canada. Tectonics 36, 1633–1659. https://doi.org/10.1002/2017TC004479.

Darbyshire, F., Eaton, D., Bastow, I., 2013. Seismic imaging of the lithosphere beneath Hudson Bay: episodic growth of the Laurentian mantle keel. Earth Planet. Sci. Lett. 373, 179–193. https://doi.org/10.1016/j.epsl.2013.05.002.

Davidson, A., 1995. A review of the Grenville orogen in its North American type area. AGSO J. Aust. Geol. Geophys. 16, 3–24.

Eaton, D., Frederiksen, A., 2007. Seismic evidence for convection-driven motion of the North American plate. Nature 446, 428–431. https://doi.org/10.1038/nature05675.

Eaton, D.W., Perry, C.H., 2013. Ephemeral isopycnicity of cratonic mantle keels. Nat. Geosci. 6, 967–970. https://doi.org/10.1038/ngeo1950.

Eeken, T., Goes, S., Pedersen, H.A., Arndt, N.T., Bouilhol, P., 2018. Seismic evidence for depth-dependent metasomatism in cratons. Earth Planet. Sci. Lett. 491, 148–159. https://doi.org/10.1016/j.epsl.2018.03.018.

Engdahl, E.R., Van der Hilst, R.D., Buland, R., 1998. Global teleseismic earthquake relocation with improved travel times and procedures for depth determination. Bull. Seismol. Soc. Am. 88, 722–743.

Frederiksen, A., Bollmann, T., Darbyshire, F., van der Lee, S., 2013. Modification of continental lithosphere by tectonic processes: a tomographic image of central North America. J. Geophys. Res. 118, 1051–1066. https://doi.org/10.1002/jgrb.50060.

Golos, E.M., Fang, H., Yao, H., Zhang, H., Burdick, S., Vernon, F., Schaeffer, A., Lebedev, S., Van der Hilst, R.D., 2018. Shear wave tomography beneath the United States using a joint inversion of surface and body waves. J. Geophys. Res. 123, 5169–5189. https://doi.org/10.1029/2017jb014894.

Griffin, W., O'Reilly, S., Doyle, B., Pearson, N., Coopersmith, H., Kivi, K., Malkovets, V., Pokhilenko, N., 2004. Lithosphere mapping beneath the North American plate. Lithos 77, 873–922. https://doi.org/10.1016/j.lithos.2004.03.034.

Harig, C., Molnar, P., Houseman, G.A., 2010. Lithospheric thinning and localization of deformation during Rayleigh-Taylor instability with nonlinear rheology and implications for intracontinental magmatism. J. Geophys. Res. 115. https://doi.org/10.1029/2009jb006422.

Hatcher, R.D., 2005. Southern and central Appalachians. In: Encyclopedia of Geology, pp. 72–81.

Hauser, E.C., 1993. Grenville foreland thrust belt hidden beneath the eastern U.S. midcontinent. Geology 21, 61–64. https://doi.org/10.1130/0091-7613(1993)021<0061:gftbhb>2.3.co;2.

Hawkesworth, C., Kempton, P., Rogers, N., Ellam, R., Calsteren, P.v., 1990. Continental mantle lithosphere, and shallow level enrichment processes in the Earth's mantle. Earth Planet. Sci. Lett. 96, 256–268. https://doi.org/10.1016/0012-821x(90)90006-j.

Heaman, L., Kjarsgaard, B., 2000. Timing of eastern North American kimberlite magmatism: continental extension of the Great Meteor hotspot track? Earth Planet. Sci. Lett. 178, 253–268. https://doi.org/10.1016/S0012-821X(00)00079-0.

Hoffman, P.F., 1991. Did the breakout of Laurentia turn Gondwanaland inside-out? Science 252, 1409–1412. https://doi.org/10.1126/science.252.5011.1409.

Jackson, J., McKenzie, D., Priestley, K., Emmerson, B., 2008. New views on the structure and rheology of the lithosphere. J. Geol. Soc. Lond. 165, 453–465. https://doi.org/10.1144/0016-76492007-109.

Jordan, T.H., 1978. Composition and development of the continental tectosphere. Nature 274, 544–548. https://doi.org/10.1038/274544a0.

Kelemen, P.B., Hart, S.R., Bernstein, S., 1998. Silica enrichment in the continental upper mantle via melt/rock reaction. Earth Planet. Sci. Lett. 164, 387–406. https://doi.org/10.1016/S0012-821X(98)00233-7.

Kennett, B.L.N., Engdahl, E.R., Buland, R., 1995. Constraints on seismic velocities in the earth from traveltimes. Geophys. J. Int. 122, 108–124. https://doi.org/10.1111/j.1365-246X.1995.tb03540.x.

Laske, G., Masters, G., 1997. A global digital map of sediment thickness. Eos Trans. AGU 78.

Li, C., Van der Hilst, R.D., Engdahl, R., Burdick, S., 2008a. A new global model for P wave speed variations in Earth's mantle. Geochem. Geophys. Geosyst. 9. https://doi.org/10.1029/2007GC001806.

Li, Z., Bogdanova, S., Collins, A., Davidson, A., Waele, B.D., Ernst, R., Fitzsimons, I., Fuck, R., Gladkochub, D., Jacobs, J., Karlstrom, K., Lu, S., Natapov, L., Pease, V., Pisarevsky, S., Thrane, K., Vernikovsky, V., 2008b. Assembly, configuration, and break-up history of Rodinia: a synthesis. Precambrian Res. 160, 179–210. https://doi.org/10.1016/j.precamres.2007.04.021.

Liao, J., Wang, Q., Gerya, T., Ballmer, M.D., 2017. Modeling craton destruction by hydration-induced weakening of the upper mantle. J. Geophys. Res. 122, 7449–7466. https://doi.org/10.1002/2017JB014157.

Liu, L., 2015. The ups and downs of North America: evaluating the role of mantle dynamic topography since the Mesozoic. Rev. Geophys. 53, 1022–1049. https://doi.org/10.1002/2015rg000489.

Ludden, J., Hynes, A., 2000. The Lithoprobe Abitibi-Grenville transect: two billion years of crust formation and recycling in the Precambrian Shield of Canada. Can. J. Earth Sci. 37, 459–476. https://doi.org/10.1139/e99-120.

Mazza, S.E., Gazel, E., Johnson, E.A., Kunk, M.J., McAleer, R., Spotila, J.A., Bizimis, M., Coleman, D.S., 2014. Volcanoes of the passive margin: the youngest magmatic event in eastern North America. Geology 42, 483–486. https://doi.org/10.1130/g35407.1.

McKenzie, D., Priestley, K., 2008. The influence of lithospheric thickness variations on continental evolution. Lithos 102, 1–11. https://doi.org/10.1016/j.lithos.2007.05.005.

McKenzie, D., Priestley, K., 2016. Speculations on the formation of cratons and cratonic basins. Earth Planet. Sci. Lett. 435, 94–104. https://doi.org/10.1016/j.epsl.2015.12.010.

Petrescu, L., Darbyshire, F., Bastow, I., Totten, E., Gilligan, A., 2017. Seismic anisotropy of Precambrian lithosphere: insights from Rayleigh wave tomography of the eastern Superior Craton. J. Geophys. Res. 122, 3754–3775. https://doi.org/10.1002/2016jb013599.

Pollitz, F.F., Mooney, W.D., 2016. Seismic velocity structure of the crust and shallow mantle of the Central and Eastern United States by seismic surface wave imaging. Geophys. Res. Lett. 43, 118–126. https://doi.org/10.1002/2015GL066637.

Priestley, K., McKenzie, D., Ho, T., 2019. A lithosphere - asthenosphere boundary - a global model derived from multimode surface-wave tomography and petrology. In: Yuan, H., Romanowicz, B. (Eds.), Lithospheric Discontinuities, 1st ed. In: Geophysical Monographs, vol. 239. American Geophysical Union and John Wiley & Sons, Inc., pp. 111–123 (Chapter 6).

Rivers, T., 1997. Lithotectonic elements of the Grenville Province: review and tectonic implications. Precambrian Res. 86, 117–154. https://doi.org/10.1016/S0301-9268(97)00038-7.

Rivers, T., 2009. The Grenville Province as a large hot long-duration collisional orogen – insights from the spatial and thermal evolution of its orogenic fronts. Geol. Soc. (Lond.) Spec. Publ. 327, 405–444. https://doi.org/10.1144/SP327.17.

Rivers, T., 2012. Upper-crustal orogenic lid and mid-crustal core complexes: signature of a collapsed orogenic plateau in the hinterland of the Grenville Province. Can. J. Earth Sci. 49, 1–42. https://doi.org/10.1139/e11-014.

Schaeffer, A., Lebedev, S., 2014. Imaging the North American continent using waveform inversion of global and USArray data. Earth Planet. Sci. Lett. 402, 26–41. https://doi.org/10.1016/j.epsl.2014.05.014.

Schmandt, B., Lin, F., 2014. P and S wave tomography of the mantle beneath the United States. Geophys. Res. Lett. 41, 6342–6349. https://doi.org/10.1002/2014GL061231.

Schutt, D., Lesher, C., 2006. Effects of melt depletion on the density and seismic velocity of garnet and spinel lherzolite. J. Geophys. Res. 111. https://doi.org/10.1029/2003JB002950.

Schutt, D.L., Lesher, C.E., 2010. Compositional trends among Kaapvaal Craton garnet peridotite xenoliths and their effects on seismic velocity and density. Earth Planet. Sci. Lett. 300, 367–373. https://doi.org/10.1016/j.epsl.2010.10.018.

Sleep, N., 2003. Survival of Archean cratonal lithosphere. J. Geophys. Res. 108. https://doi.org/10.1029/2001JB000169.

Sloan, R.A., Jackson, J.A., McKenzie, D., Priestley, K., 2011. Earthquake depth distributions in central Asia, and their relations with lithosphere thickness, shortening and extension. Geophys. J. Int. 185, 1–29. https://doi.org/10.1111/j.1365-246x.2010.04882.x.

Stein, C.A., Stein, S., Elling, R., Keller, R., Kley, J., 2017. Is the "Grenville Front" in the central United States really the Midcontinent Rift? GSA Today 28. https://doi.org/10.1130/gsatg357a.1.

Tesauro, M., Kaban, M.K., Mooney, W.D., Cloetingh, S., 2014. NACr14: a 3D model for the crustal structure of the North American Continent. Tectonophysics 631, 65–86. https://doi.org/10.1016/j.tecto.2014.04.016.

Wagner, L.S., Anderson, M.L., Jackson, J.M., Beck, S.L., Zandt, G., 2008. Seismic evidence for orthopyroxene enrichment in the continental lithosphere. Geology 36, 935–938. https://doi.org/10.1130/g25108a.1.

Wenker, S., Beaumont, C., 2018. Can metasomatic weakening result in the rifting of cratons? Tectonophysics 746, 3–21. https://doi.org/10.1016/j.tecto.2017.06.013.

Whitmeyer, S.J., Karlstrom, K.E., 2007. Tectonic model for the Proterozoic growth of North America. Geosphere 3, 220–259. https://doi.org/10.1130/ges00055.1.

Yuan, H., Romanowicz, B., 2010. Lithospheric layering in the North American craton. Nature 466, 1063–1068. https://doi.org/10.1111/j.1365-246X.2010.04901.x.